

# Ironing out primordial temperature fluctuations with polarisation: optimal detection of cosmic structure imprints

M. Frommert & T. A. Enßlin

*Max-Planck-Institut für Astrophysik, Karl-Schwarzschild-Straße 1, D-85748 Garching b. München, Germany  
mona@mpa-garching.mpg.de*

Accepted ??? Received ???; in original form ???

## ABSTRACT

Secondary anisotropies of the cosmic microwave background (CMB) can be detected by using the cross-correlation between the large-scale structure (LSS) and the CMB temperature fluctuations. In such studies, chance correlations of primordial CMB fluctuations with the LSS are the main source of uncertainty. We present a method for reducing this noise by exploiting information contained in the polarisation of CMB photons. The method is described in general terms and then applied to our recently proposed optimal method for measuring the integrated Sachs-Wolfe (ISW) effect. We obtain an expected signal-to-noise ratio of up to 8.5. This corresponds to an enhancement of the signal-to-noise by 23 per cent as compared to the standard method for ISW detection, and by 16 per cent w.r.t. our recently proposed method, both for the best-case scenario of having perfect (noiseless) CMB and LSS data.

**Key words:** Cosmology: CMB – Large-Scale Structure

## 1 INTRODUCTION

The low-redshift large-scale structure (LSS) changes the cosmic microwave background (CMB) fluctuations in various ways. Such secondary effects on the CMB are, for example, the integrated Sachs-Wolfe (ISW) effect (Sachs & Wolfe 1967), the Rees-Sciama (RS) effect (Rees & Sciama 1968), gravitational lensing (Lewis & Challinor 2006), and the Sunyaev-Zel'dovich (SZ) effect (Sunyaev & Zeldovich 1972, 1980). By studying these signals, we can obtain valuable information about our Universe. The ISW effect, for example, provides independent evidence for the existence of dark energy. Unfortunately, unless the spectral signatures of the signal differ from the ones of the primordial CMB, it is difficult to detect them. The reason is that the primordial CMB fluctuations created at the time of last scattering are much stronger than the secondary temperature anisotropies. The usual method for detecting secondary anisotropies in the CMB is via cross-correlating the CMB temperature maps with LSS data such as the galaxy density contrast. Since secondary anisotropies in the CMB are created by the LSS, there is a significant cross-correlation between the two. In contrast, the primordial CMB fluctuations should not be correlated with the LSS. By performing the cross-correlation analysis, one can therefore separate signatures of the presence of these secondary anisotropies from the primordial fluctuations.

In the standard cross-correlation method, first described by Boughn et al. (1998), the observed cross-correlation between LSS and CMB data is compared to its theoretical prediction. This method has been extensively used to detect the ISW effect. Some of the most recent studies are by Ho et al. (2008), Giannantonio et al.

(2008), Rassat et al. (2006), and Boughn & Crittenden (2004). Since the theoretical cross-correlation function is by construction an ensemble average over all possible universes, fluctuations associated with the specific realisation of the LSS in the observed Universe act as a source of noise in the detected signal in the standard method.

In Frommert et al. (2008), we suggested a method for reducing this source of uncertainty, which we will refer to as the optimal temperature-only method. Instead of comparing the observed cross-correlation function with its theoretical prediction, we use an optimal matched filter in order to detect an ISW template in CMB data. Similar schemes were independently proposed by Zhang (2006), Hernández-Monteagudo (2008) and Granett et al. (2008). Optimal matched filters have also been used to study other secondary effects on the CMB. The first of these studies explored the detectability of the kinetic SZ effect of galaxy clusters (Haehnelt & Tegmark 1996), later works on the kinetic SZ effect and the RS effect are for example by Schäfer et al. (2006), Maturi et al. (2007a), Maturi et al. (2007b), and Waelkens et al. (2008).

However, in both the standard method and the optimal temperature-only method, the main source of uncertainty in the detection of the secondary signal comes from chance correlations of primordial CMB fluctuations with the LSS. In this work, we present a method which exploits polarisation information in order to reduce not only the noise from the specific LSS realisation, but also the noise coming from primordial CMB temperature fluctuations. This method can be applied generically to the detection of all secondary effects. It is based on the fact that the polarisation measured in the

arXiv:0811.4433v2 [astro-ph] 26 Feb 2009

CMB contains information about the primordial temperature fluctuations. We use the observed E-mode polarisation map, which we translate into a temperature map using the TE cross-power spectrum. The obtained temperature map is then subtracted from the observed temperature map, and hence no longer contributes to the noise budget of the detected signal. Once an E-map has been measured to a good accuracy, this will significantly enhance the signal-to-noise ratio of the detection of secondary effects. The first all-sky measurement of polarisation with high fidelity is expected to be provided by the Planck Surveyor satellite (Tauber 2000), to be launched in 2009.

Our optimal polarisation method builds on the optimal scheme to detect LSS signatures in CMB data, which we developed in Frommert et al. (2008) specifically for the ISW effect. Note that this method assumes a Gaussian data model, hence it is very well suited for the ISW effect, whereas one might need to extend it into the non-Gaussian regime for other effects, such as the RS effect, the kinetic SZ effect or lensing. This can be done using information field theory (Enßlin et al. 2008), but is beyond the scope of this work. Here we show how to use the information contained in polarisation data within the framework of a Gaussian data model and leave the extension to more complicated models for future work.

When applying our method to ISW detection, we obtain an expected signal-to-noise ratio of up to 8.5. This corresponds to an enhancement of the signal-to-noise ratio by 16 per cent w.r.t. the optimal temperature-only method, independent of the depth of the galaxy survey considered. In comparison to the standard method, the signal-to-noise ratio is enhanced by 23 per cent for a full-sky LSS survey that goes out to redshift 2. Both of these comparisons have been made for the best-case scenario of having perfect (noise-less) CMB and LSS data.

Using polarisation data to reduce the noise in the detection of secondary effects was first proposed by Robert Crittenden, following a suggestion from Lyman Page (Crittenden 2006). He already derived the reduced temperature power spectrum, which we show in Figure 1, and roughly estimates the improvement of the signal-to-noise ratio for ISW detection to be around 20 per cent, which we confirm with our calculations.

Our article is organised as follows. In section 2 we describe the optimal method derived in Frommert et al. (2008) in general terms. In section 3 we then show how we can reduce the noise coming from primordial temperature fluctuations by using polarisation data. In section 4, we apply the method to the ISW effect. We conclude in section 5.

## 2 OPTIMAL METHOD FOR THE DETECTION OF SECONDARY EFFECTS ON THE CMB

In Frommert et al. (2008), we derived an optimal method for the detection of secondary temperature anisotropies in the CMB using as example the ISW effect. In this section we briefly review this method, which we refer to as the optimal temperature-only method.

Let's assume that we know the LSS well enough to create a template  $T_\tau$  of the secondary signal  $T_s$  that we would like to detect in the temperature fluctuations, for example the ISW signal  $T_{\text{isw}}$ . Here,  $T_X$  with any index  $X$  denotes the function  $T_X : S^2 \rightarrow \mathbb{R}$ , which we regard also as an element of a function-vector space. The data  $d$  we measure are the observed CMB temperature fluctuations  $T_{\text{obs}}$ . Our data model is then

$$d \equiv T_{\text{obs}}$$

Symbol	Definition
$T_{\text{cmb}}, E_{\text{cmb}}$	cosmological CMB temperature and polarisation
$T_s, E_s$	real secondary signal that we are trying to detect
$T_\tau, E_\tau$	signal templates for temperature and polarisation
$T_{\text{fg}}, E_{\text{fg}}$	residual galactic foregrounds after foreground removal
$T_{\text{det}}, E_{\text{det}}$	detector noise
$T_{\text{obs}}, E_{\text{obs}}$	$(T_{\text{cmb}} + T_{\text{fg}} + T_{\text{det}}), (E_{\text{cmb}} + E_{\text{fg}} + E_{\text{det}})$
$\Delta T_{\text{obs}}, \Delta E_{\text{obs}}$	$(T_{\text{obs}} - T_\tau), (E_{\text{obs}} - E_\tau)$
$T_{\text{isw}}$	fluctuations created by ISW effect
$T_{\text{prim}}$	$(T_{\text{cmb}} - T_{\text{isw}})$

**Table 1.** Summary of defined symbols

$$\begin{aligned} &= T_{\text{cmb}} + T_{\text{fg}} + T_{\text{det}} \\ &= T_\tau + (T_{\text{cmb}} - T_\tau) + T_{\text{fg}} + T_{\text{det}} \\ &\equiv T_\tau + \Delta T_{\text{obs}}, \end{aligned} \quad (1)$$

where  $T_{\text{cmb}}$  denotes the cosmological CMB temperature fluctuations,  $T_{\text{fg}}$  are residual galactic foregrounds after foreground-removal, and  $T_{\text{det}}$  denotes the detector noise. Note that  $(T_{\text{cmb}} - T_\tau) = (T_{\text{cmb}} - T_s) + (T_s - T_\tau)$  contains the the CMB fluctuations other than the signal we are after,  $(T_{\text{cmb}} - T_s)$ , and the uncertainty in the template w.r.t. the signal,  $(T_s - T_\tau)$ , coming from our ignorance of the full distribution of the matter in the Universe. Note that for simplifying the notation, we have redefined  $T \equiv (T - T_0)/T_0$ , where  $T_0$  denotes the monopole of the CMB temperature fluctuations. An overview over the above definitions can be found in table 1.

We now approximate the distribution of  $\Delta T_{\text{obs}}$  by a Gaussian around zero. That is, we write the probability density function of  $T_{\text{obs}}$  given the signal template  $T_\tau$  and the cosmological parameters  $p$ , the likelihood, as

$$P(T_{\text{obs}} | T_\tau, p) = \mathcal{G}(T_{\text{obs}} - T_\tau, C). \quad (2)$$

Here we have defined

$$\mathcal{G}(\chi, C) \equiv \frac{1}{\sqrt{|2\pi C|}} \exp\left(-\frac{1}{2}\chi^\dagger C^{-1}\chi\right) \quad (3)$$

to denote the probability density function of a Gaussian distributed vector  $\chi$  with zero mean, given the cosmological parameters  $p$  and the covariance matrix  $C \equiv \langle \chi\chi^\dagger \rangle$ , where the averages are taken over the Gaussian distribution  $\mathcal{G}(\chi, C)$ . Note that in general the covariance matrix depends on the cosmological parameters, which is not explicitly stated in our notation. A daggered vector or matrix denotes its transposed and complex conjugated version, as usual. Hence, given two vectors  $a$  and  $b$ ,  $a b^\dagger$  must be read as the tensor product, whereas  $a^\dagger b$  denotes the scalar product. Note that in eq. (2) the signal template  $T_\tau$  may depend on the cosmological parameters  $p$  as well.

Let us briefly address the question of how to create the template  $T_\tau$ . When writing down the likelihood in eq. (2), we have implicitly assumed that the template  $T_\tau$  is the mean of  $T_{\text{obs}}$  w.r.t. the probability distribution given in eq. (2). This probability distribution is conditional on the template  $T_\tau$ , or, in other words, conditional on the LSS data  $\delta_g$ , from which we have created our template according to some prescription. Note that usually  $\delta_g$  denotes the galaxy density contrast, but we use it to denote the LSS data in a more general sense here, which could also be lensing information, for example.

In the following, we assume that the signal  $T_s = R\delta_m$  is given by a linear operator  $R$  applied to the matter density contrast  $\delta_m$ . For the ISW effect, the operator  $R$  is explicitly derived in

Frommert et al. (2008). We can then write

$$\begin{aligned} T_\tau &\equiv \langle T_{\text{obs}} \rangle_{P(T_{\text{obs}} | \delta_{g,p})} \\ &\approx \langle T_s \rangle_{P(T_s | \delta_{g,p})} + \langle (T_{\text{cmb}} - T_s) \rangle_{P((T_{\text{cmb}} - T_s) | \delta_{g,p})} \\ &\quad + \langle T_{\text{fg}} \rangle_{P(T_{\text{fg}} | \delta_{g,p})} + \langle T_{\text{det}} \rangle_{P(T_{\text{det}})} \\ &= R \langle \delta_m \rangle_{P(\delta_m | \delta_{g,p})}, \end{aligned} \quad (4)$$

where we have used that  $T_s$ ,  $(T_{\text{cmb}} - T_s)$ ,  $T_{\text{fg}}$  and  $T_{\text{det}}$  are approximately stochastically independent in the first step, and that the three errors have vanishing means,  $\langle (T_{\text{cmb}} - T_s) \rangle_{P((T_{\text{cmb}} - T_s) | \delta_{g,p})} = \langle T_{\text{fg}} \rangle_{P(T_{\text{fg}} | \delta_{g,p})} = \langle T_{\text{det}} \rangle_{P(T_{\text{det}})} = 0$ , in the second step. For the ISW effect,  $(T_{\text{cmb}} - T_s) \equiv (T_{\text{cmb}} - T_{\text{isw}}) = T_{\text{prim}}$  are simply the primordial fluctuations, which do have zero mean (Frommert et al. 2008). For other secondary effects,  $\langle (T_{\text{cmb}} - T_s) \rangle_{P((T_{\text{cmb}} - T_s) | \delta_{g,p})} = 0$  is probably still a reasonably good approximation. In the last step, we have pulled the operator  $R$  out of the mean.

We see that for creating the signal template  $T_\tau$ , we need the mean of the matter density contrast conditional on the LSS data,  $\langle \delta_m \rangle_{P(\delta_m | \delta_{g,p})}$ . In the simplest case of having a Gaussian likelihood and Gaussian prior for  $\delta_m$ , this is given by the Wiener filter. Again this is a very good approximation for the ISW effect, which is present on very large scales, on which structure growth is still linear. For other effects such as the kinetic SZ effect, the RS effect or lensing, the Gaussian approximation for  $\delta_m$  may not be very good (thus also the Gaussian approximation for  $\Delta T_{\text{obs}}$  may not be good), and one would have to consider non-Gaussian data models using information field theory (Enßlin et al. 2008). However, in this work we will use the Gaussian data model and leave extensions to non-Gaussian models for future work. Note that, when choosing the template as in eq. (4), the latter is uncorrelated with  $\Delta T_{\text{obs}} \equiv (T_{\text{obs}} - T_\tau)$  (w.r.t. the probability distribution in eq. (2)), as can be easily shown.

In order to see how well we can recover such a signal template from the CMB data, we put an amplitude  $A_\tau$  in front of the signal  $T_\tau$  in eq. (2), and try to estimate its value from the data (the true value of this amplitude is one, of course):

$$P(T_{\text{obs}} | A_\tau, T_\tau, p) = \mathcal{G}(T_{\text{obs}} - A_\tau T_\tau, C). \quad (5)$$

The maximum likelihood estimator  $\hat{A}_\tau$  for the amplitude  $A_\tau$  is

$$\hat{A}_\tau = \frac{T_{\text{obs}}^\dagger C^{-1} T_\tau}{T_\tau^\dagger C^{-1} T_\tau} = \frac{\sum_l (2l+1) \frac{\hat{C}_l^{T_\tau, T_{\text{obs}}}}{C_l^{\Delta T_{\text{obs}}}}}{\sum_l (2l+1) \frac{\hat{C}_l^{T_\tau}}{C_l^{\Delta T_{\text{obs}}}}}. \quad (6)$$

In the second equality, we have assumed that the knowledge of the secondary anisotropy template is equally good in any direction, so that the template uncertainty matrix is isotropic and fully described by its spherical harmonics power spectrum. We will use this assumption also in the following. This permits us to evaluate the expressions in spherical harmonics space in the second step. We have used the following definitions of the power spectra and their estimators (we use a hat to denote estimators)

$$C_l^{X,Y} \equiv \langle a_{lm}^X a_{lm}^{Y*} \rangle, \quad (7)$$

$$C_l^X \equiv C_l^{X,X}, \quad (8)$$

$$\hat{C}_l^{X,Y} \equiv \frac{1}{2l+1} \sum_l \text{Re} \left( a_{lm}^X a_{lm}^{Y*} \right), \quad (9)$$

$$\hat{C}_l^X \equiv \hat{C}_l^{X,X}, \quad (10)$$

where the  $a_{lm}$  are defined by an expansion into spherical harmonics  $Y_{lm}$ :

$$a_{lm}^X \equiv \int_S d\Omega T_X(\hat{n}) Y_{lm}^*(\hat{n}). \quad (11)$$

The power spectrum  $C_l^{\Delta T_{\text{obs}}}$  denotes the spherical harmonics space version of the covariance matrix  $C$ . We calculate the variance of the amplitude estimator to be

$$\begin{aligned} \sigma_A^2 &\equiv \langle (\hat{A}_\tau - \langle \hat{A}_\tau \rangle_{\text{cond}})^2 \rangle_{\text{cond}} \\ &= \left( T_\tau^\dagger C^{-1} T_\tau \right)^{-1} = \left( \sum_l (2l+1) \frac{\hat{C}_l^{T_\tau}}{C_l^{\Delta T_{\text{obs}}}} \right)^{-1}, \end{aligned} \quad (12)$$

where we have again evaluated the expressions in spherical harmonics space in the last step, and we have used the notation introduced in Frommert et al. (2008), where the index ‘‘cond’’ indicates that the average is taken conditional on the signal template  $T_\tau$ , i.e. over the probability distribution given in eq. (2). We can now define the signal-to-noise ratio as follows

$$\left( \frac{S}{N} \right)_t \equiv \frac{1}{\sigma_A^2} = \sum_l (2l+1) \frac{\hat{C}_l^{T_\tau}}{C_l^{\Delta T_{\text{obs}}}}, \quad (13)$$

where the index  $t$  indicates that this is the signal-to-noise ratio one obtains for the optimal temperature-only method. This signal-to-noise ratio depends on the actual realisation of the matter distribution in our Universe via the estimator  $\hat{C}_l^{T_\tau}$ . In Frommert et al. (2008), we showed that for the ISW effect we obtain on average a signal-to-noise ratio of about 7, if we assume an ideal LSS survey which covers the whole sky and goes out to a redshift of about 2. In comparison to the standard method, this is an enhancement of the signal-to-noise ratio by about 7 per cent.

### 3 REDUCTION OF THE PRIMORDIAL NOISE USING POLARISATION INFORMATION

With the method suggested in Frommert et al. (2008), we were able to reduce the low redshift cosmic variance effect in amplitude estimates of secondary signals, i.e. we reduced the noise coming from the specific realisation of LSS in our Universe. Now we show how even the noise coming from primordial temperature fluctuations can be reduced. The idea is that since the temperature and polarisation maps of the CMB are correlated, the polarisation contains information about the temperature fluctuations. After extracting this information from the polarisation data we know a part of the temperature map, which we can remove from the data before trying to detect the signal. In other words, we make our amplitude estimate of the secondary signal conditional on the known part of the temperature fluctuations.

To include the information contained in the polarisation data, we enlarge our data vector  $d$  to include the observed E-mode polarisation map  $E_{\text{obs}}$  as well:

$$d \equiv (T_{\text{obs}}, E_{\text{obs}})^\dagger, \quad (14)$$

or, in spherical harmonics space

$$a_{lm}^d \equiv \left( a_{lm}^{T_{\text{obs}}}, a_{lm}^{E_{\text{obs}}} \right)^\dagger. \quad (15)$$

Note that with *the map*  $E_{\text{obs}}$ , we are referring again to the abstract element of a function-vector space space, which contains all the information on the observed E-mode. When evaluating the abstract expressions obtained in the following, we use the representation of  $E_{\text{obs}}$  in spherical harmonics space, consisting of all coefficients  $a_{lm}^{E_{\text{obs}}}$ .

In principle, it is possible that the secondary effect we are looking for is also present as a small signal in the polarisation data. If the temperature anisotropies created by the secondary effect exhibit a quadrupole component at the time of reionization, this quadrupole will be rescattered by free electrons and create a polarisation signal (Zaldarriaga 1997). However, for the ISW this effect has been proven to be small (Cooray & Melchiorri 2006). It should also be small for the RS effect, lensing and the kinetic SZ effect, the highest contributions of which are on relatively small scales. Thus, as a first approximation we assume that the polarisation data do not carry any signal of the effect we want to detect. Our signal template  $\tau$  is then

$$\begin{aligned}\tau &\equiv (T_\tau, 0)^\dagger, \\ a_{lm}^\tau &\equiv (a_{lm}^{T_\tau}, 0)^\dagger,\end{aligned}\quad (16)$$

and the data model becomes

$$d = \begin{pmatrix} T_{\text{obs}} \\ E_{\text{obs}} \end{pmatrix} = \begin{pmatrix} T_\tau + \Delta T_{\text{obs}} \\ E_{\text{obs}} \end{pmatrix}. \quad (17)$$

The observed E-map,  $E_{\text{obs}} = E_{\text{cmb}} + E_{\text{fg}} + E_{\text{det}}$ , consists of the cosmological E-mode fluctuations  $E_{\text{cmb}}$ , residual galactic foregrounds after foreground removal  $E_{\text{fg}}$ , and the detector noise  $E_{\text{det}}$ . Assuming again Gaussianity, we can write down the likelihood

$$P(d|\tau, p) = \mathcal{G}(d - \tau, \tilde{C}), \quad (18)$$

where the covariance matrix  $\tilde{C}$  is

$$\tilde{C} \equiv \langle (d - \tau)(d - \tau)^\dagger \rangle_{\text{cond}}, \quad (19)$$

and we have redefined the index 'cond' to denote the average over the probability distribution in eq. (18). In spherical harmonics space, the covariance matrix  $\tilde{C}$  is block-diagonal with the blocks being

$$\tilde{C}(l) = \begin{pmatrix} C_l^{\Delta T_{\text{obs}}} & C_l^{\Delta T_{\text{obs}}, E_{\text{obs}}} \\ C_l^{\Delta T_{\text{obs}}, E_{\text{obs}}} & C_l^{E_{\text{obs}}} \end{pmatrix}. \quad (20)$$

Therefore, the likelihood factorises:

$$P(d|\tau, p) = \prod_{l,m} \mathcal{G}(a_{lm}^d - a_{lm}^\tau, \tilde{C}(l)). \quad (21)$$

When inserting the inverse of the covariance matrix  $\tilde{C}(l)$ , it is possible to rewrite the likelihood as a product of a reduced temperature part and a polarisation part. To this end, let us define the reduced temperature map and power spectrum

$$\begin{aligned}a_{lm}^{T_{\text{red}}} &\equiv a_{lm}^{T_{\text{obs}}} - \frac{C_l^{\Delta T_{\text{obs}}, E_{\text{obs}}}}{C_l^{E_{\text{obs}}}} a_{lm}^{E_{\text{obs}}}, \\ C_l^{\text{red}} &\equiv C_l^{\Delta T_{\text{obs}}} - \frac{(C_l^{\Delta T_{\text{obs}}, E_{\text{obs}}})^2}{C_l^{E_{\text{obs}}}}.\end{aligned}\quad (22)$$

With these definitions, the likelihood becomes

$$P(d|\tau, p) = \prod_{l,m} \left[ \mathcal{G}(a_{lm}^{T_{\text{red}}} - a_{lm}^\tau, C_l^{\text{red}}) \mathcal{G}(a_{lm}^{E_{\text{obs}}}, C_l^{E_{\text{obs}}}) \right], \quad (23)$$

as we prove in Appendix A. Now our goal is to find the signal template  $T_\tau$  in the CMB data. The polarisation part of the above likelihood,  $\mathcal{G}(a_{lm}^{E_{\text{obs}}}, C_l^{E_{\text{obs}}})$ , does not depend on the signal template, nor does the reduced temperature part explicitly depend on  $E_{\text{obs}}$ . In other words, the observed E-map does not contain relevant information any more after introducing the reduced temperature fluctuations. Thus, we can marginalize over it, and continue only with

the likelihood of the reduced temperature map

$$\begin{aligned}P(T_{\text{red}} | T_\tau, p) &\equiv \mathcal{G}(T_{\text{red}} - T_\tau, C_{\text{red}}) \\ &= \prod_{l,m} \mathcal{G}(a_{lm}^{T_{\text{red}}} - a_{lm}^{T_\tau}, C_l^{\text{red}}).\end{aligned}\quad (24)$$

Note that it is straightforward to derive the factorised likelihood also for the case that we do have a non-zero signal template  $E_\tau$  for the polarisation part. In that case, the covariance matrix  $\tilde{C}(l)$  is slightly changed, as well as the definitions of the reduced temperature map and power spectrum, and we can no longer neglect the polarisation part of the likelihood. Please refer to Appendix A for details.

Let us pause for a second and have a closer look at the quantities defined in eq. (22). What we have effectively done is the following. We have a polarisation map  $a_{lm}^{E_{\text{obs}}}$ , which is correlated with the temperature fluctuations  $a_{lm}^{\Delta T_{\text{obs}}}$  via  $C_l^{\Delta T_{\text{obs}}, E_{\text{obs}}}$ . That is, the polarisation map contains information about the temperature map, which we can translate into a 'known' part of the temperature map using the prescription  $(C_l^{\Delta T_{\text{obs}}, E_{\text{obs}}}/C_l^{E_{\text{obs}}}) a_{lm}^{E_{\text{obs}}}$ . This known part of the temperature map is subtracted from the observed one, and we work only with the remaining unknown temperature fluctuations in which we try to detect our signal template.

The reduced temperature map fluctuates around our signal template  $T_\tau$  only with the variance  $C_l^{\text{red}}$ , which is smaller than the full variance  $C_l^{\Delta T_{\text{obs}}}$  of the observed temperature map. This reduced variance is the uncertainty going into our signal detection problem now, rather than the full variance of the original temperature fluctuations.

In order to see this, let us again put an amplitude in front of the signal template in eq. (24), and estimate it from the data using a maximum likelihood estimator:

$$\hat{A}_\tau = \frac{T_{\text{red}}^\dagger C_{\text{red}}^{-1} T_\tau}{T_\tau^\dagger C_{\text{red}}^{-1} T_\tau} = \frac{\sum_l (2l+1) \frac{\hat{C}_l^{T_{\text{red}}, T_\tau}}{C_l^{\text{red}}}}{\sum_l (2l+1) \frac{\hat{C}_l^{T_\tau}}{C_l^{\text{red}}}}. \quad (25)$$

Here, the last expression is in spherical harmonics space. The variance of  $\hat{A}_\tau$  is now

$$\sigma_A^2 = (T_\tau^\dagger C_{\text{red}}^{-1} T_\tau)^{-1} = \left( \sum_l (2l+1) \frac{\hat{C}_l^{T_\tau}}{C_l^{\text{red}}} \right)^{-1}, \quad (26)$$

and hence the signal-to-noise ratio becomes

$$\begin{aligned}\left(\frac{S}{N}\right)_{\text{pol}}^2 &= \sum_l (2l+1) \frac{\hat{C}_l^{T_\tau}}{C_l^{\text{red}}} \\ &= \sum_l \frac{(2l+1) \hat{C}_l^{T_\tau}}{C_l^{\Delta T_{\text{obs}}} - (C_l^{\Delta T_{\text{obs}}, E_{\text{obs}}})^2 / C_l^{E_{\text{obs}}}}.\end{aligned}\quad (27)$$

Note that we have added the index "pol" to indicate that this is the signal-to-noise ratio one obtains when using the polarisation data to reduce the variance. Comparing the signal-to-noise ratio in eq. (27) with the one in eq. (13), we see that by including the information contained in the polarisation data, we reduce the variance in every mode by the term  $(C_l^{\Delta T_{\text{obs}}, E_{\text{obs}}})^2 / C_l^{E_{\text{obs}}}$ .

Let us now get an impression of how much the variance gets reduced for the different multipoles. To this end, we neglect the detector noise  $T_{\text{det}}$  and  $E_{\text{det}}$ , and the foreground noise  $T_{\text{fg}}$  and

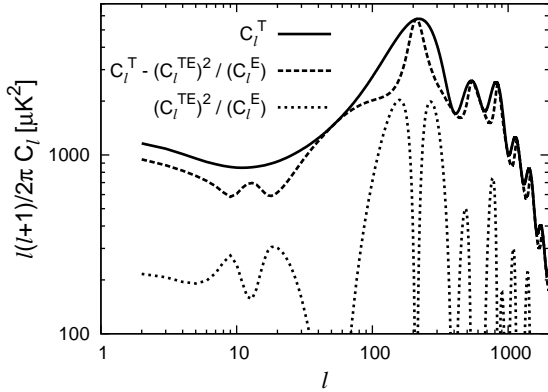


**Figure 1.** Reduction of the variance in the detection of secondary temperature signals by using the information contained in polarisation data. Shown are the CMB temperature power spectrum  $C_l^{T_{\text{cmb}}}$  (solid), and the template-free part of the reduced temperature power spectrum  $C_l^{T_{\text{cmb}}} - (C_l^{T_{\text{cmb}}, E_{\text{cmb}}})^2 / C_l^{E_{\text{cmb}}}$  (dashed), together with the part of the CMB power spectrum coming from the 'known' part of the temperature fluctuations which we infer from the polarisation map,  $(C_l^{T_{\text{cmb}}, E_{\text{cmb}}})^2 / C_l^{E_{\text{cmb}}}$  (dotted).

$E_{\text{fg}}^{-1}$ , which allows us write

$$C_l^{\Delta T_{\text{obs}}, E_{\text{obs}}} \approx C_l^{T_{\text{cmb}}, E_{\text{cmb}}} - C_l^{T_{\tau}, E_{\text{cmb}}} \quad (28)$$

$$C_l^{\Delta T_{\text{obs}}} \approx C_l^{T_{\text{cmb}}} - 2C_l^{T_{\text{cmb}}, T_{\tau}} + C_l^{T_{\tau}} \quad (29)$$

We furthermore neglect the cross-term  $C_l^{T_{\tau}, E_{\text{cmb}}}$ . For the ISW effect, we have verified numerically that it is negligible. For the kinetic SZ and RS effects, the template itself is so small that we can also certainly neglect  $C_l^{T_{\tau}, E_{\text{cmb}}}$ . Then, the reduced temperature power spectrum defined in eq. (22) becomes

$$C_l^{\text{red}} \approx C_l^{T_{\text{cmb}}} - 2C_l^{T_{\text{cmb}}, T_{\tau}} + C_l^{T_{\tau}} - \frac{(C_l^{T_{\text{cmb}}, E_{\text{cmb}}})^2}{C_l^{E_{\text{cmb}}}}. \quad (30)$$

In Fig. 1, we plot the template-free part of the reduced temperature power spectrum  $C_l^{T_{\text{cmb}}} - (C_l^{T_{\text{cmb}}, E_{\text{cmb}}})^2 / C_l^{E_{\text{cmb}}}$  (note that we have not included the template-dependent terms  $-2C_l^{T_{\text{cmb}}, T_{\tau}}$  and  $C_l^{T_{\tau}}$  in the plot), which gives us an impression of how the variance coming from primordial temperature fluctuations is being reduced by including polarisation data. The variance will be further reduced by working conditional on the signal template  $T_{\tau}$ , which is encoded in the terms  $-2C_l^{T_{\text{cmb}}, T_{\tau}}$  and  $C_l^{T_{\tau}}$ , and already described in Frommert et al. (2008). We also plot the original CMB power spectrum  $C_l^{T_{\text{cmb}}}$  and the difference to the reduced one for comparison. We have assumed a flat  $\Lambda$ CDM model with the parameter values given by Komatsu et al. (2008), table 1 ( $\Omega_b h^2 = 0.02265$ ,  $\Omega_{\Lambda} = 0.721$ ,  $h = 0.701$ ,  $n_s = 0.96$ ,  $\tau = 0.084$ ,  $\sigma_8 = 0.817$ ), and used CMBEASY ([www.cmbeasy.org](http://www.cmbeasy.org), Doran 2005) for obtaining the respective spectra.

In Fig. 2, we plot a realisation of the original temperature map  $T_{\text{cmb}}$  (top panel), the reduced temperature map  $T_{\text{red}}$  (middle panel)

<sup>1</sup> In reality, galactic E-mode foregrounds  $E_{\text{fg}}$  are likely to be the limiting factor in the improvement of the detection significance coming from including polarisation data. We comment on this at the end of this section.

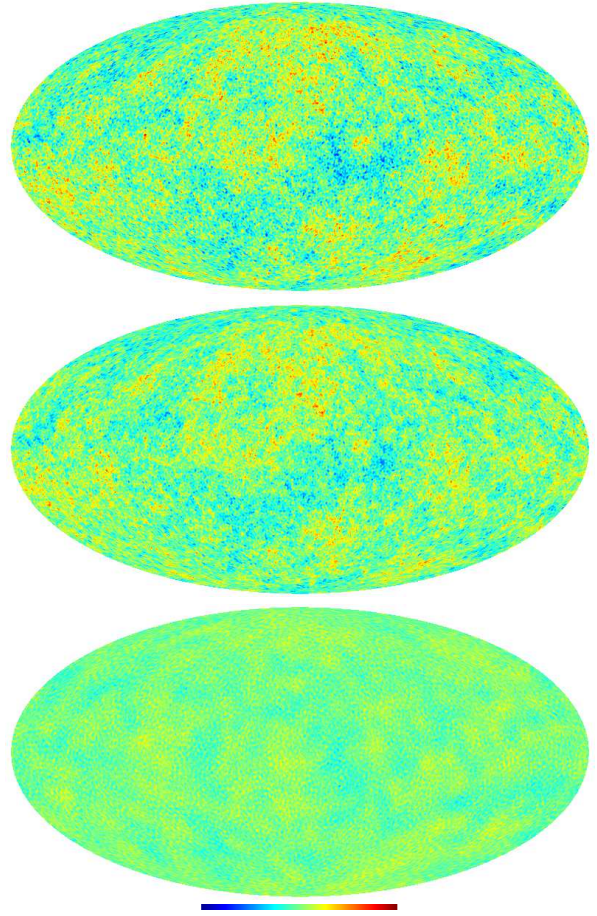


**Figure 2.** Realisation of the original CMB temperature map  $T_{\text{cmb}}$  (top panel), the reduced temperature map  $T_{\text{red}}$  (middle panel) and the difference between the two for comparison (bottom panel) in  $\mu\text{K}$ . We have chosen the same colour range from  $-500\mu\text{K}$  to  $500\mu\text{K}$  for all maps.

and the difference of the two,  $(C_l^{\Delta T_{\text{obs}}, E_{\text{obs}}} / C_l^{E_{\text{obs}}}) a_{lm}^{E_{\text{obs}}}$ , for comparison (bottom panel). The realisations were created using the HEALPix package (Górski et al. 2005).

Note that all of what we have done works equally well for reducing the E-mode polarisation map when trying to detect a secondary signal contained in the polarisation data. One has to simply exchange the roles of  $T$  and  $E$  in the derivation. This was partly already done by Jaffe (2003), who used the information contained in the CMB temperature map for predicting a polarisation map from it. The equivalent plot to Fig. 1 for this scenario is given in Fig. 3. The likelihood for the case of simultaneously detecting a temperature template  $T_{\tau}$  and a polarisation template  $E_{\tau}$  is derived in Appendix A.

In practice, the accuracy to which we can measure the E-map is limited by galactic foregrounds  $E_{\text{fg}}$ , the most important of which are synchrotron radiation and dust emission of the Milky Way. Uncertainty in the measured E-map makes the reduction of the temperature power spectrum less efficient, because the power contained in the foreground noise,  $C_l^{E_{\text{fg}}}$ , enhances the observed E-mode power spectrum  $C_l^{E_{\text{obs}}} \approx C_l^{E_{\text{cmb}}} + C_l^{E_{\text{fg}}} + C_l^{E_{\text{det}}}$ . The prediction of a realistic signal-to-noise ratio for our method would require a detailed study of foreground effects, detector noise, and scanning strategies, which is beyond the scope of this work.

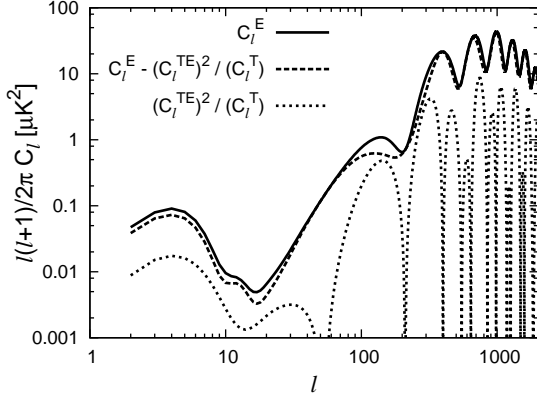


**Figure 3.** Reduction of the variance in the detection of secondary polarisation signals by using the information contained in temperature data. Shown are the CMB E-mode power spectrum  $C_l^{E_{\text{cmb}}}$  (solid), and the template-free part of the reduced E-mode power spectrum  $C_l^{E_{\text{cmb}}} - (C_l^{T_{\text{cmb},E_{\text{cmb}}}})^2 / C_l^{T_{\text{cmb}}}$  (dashed), together with the part of the CMB power spectrum coming from the ‘known’ part of the E-mode fluctuations which we infer from the temperature map,  $(C_l^{T_{\text{cmb},E_{\text{cmb}}}})^2 / C_l^{T_{\text{cmb}}}$  (dotted).

#### 4 EXAMPLE: THE ISW EFFECT

Let us now apply our method to the ISW effect. That is, our signal template  $T_\tau$  is now an ISW template which we obtain from a Wiener filter reconstruction of the LSS, which can be shown to be optimal for the purpose of ISW detection (Frommert et al. 2008). We assume the best-case scenario of having perfect (noiseless) LSS and CMB data. In other words, we neglect the detector noise  $T_{\text{det}}$  and  $E_{\text{det}}$ , which is safe on the largest scales, where cosmic variance dominates (Afshordi 2004). We furthermore neglect residual galactic foregrounds  $T_{\text{fg}}$  and  $E_{\text{fg}}$  as well as the shot-noise in the observed galaxy distribution, and assume that we have an ideal galaxy survey that covers the whole sky and goes out to a redshift of at least two. Then our signal template is exact,  $T_\tau = T_s \equiv T_{\text{isw}}$ , and the residual  $(T_{\text{cmb}} - T_{\text{isw}}) \equiv T_{\text{prim}}$  is simply given by the primordial CMB fluctuations, which are created at the surface of last scattering (we have ignored other secondary effects here). We further assume  $T_{\text{isw}}$  to be uncorrelated with the primordial fluctuations  $T_{\text{prim}}$ , which is a safe assumption because they are created on very different scales (Boughn et al. 1998). We can then write  $C_l^{T_{\text{cmb},T_\tau}} \equiv C_l^{T_{\text{cmb},T_{\text{isw}}}} = C_l^{T_{\text{isw}}}$ .

The signal-to-noise ratio for the detection of the ISW signal, eq. (27), then reduces to

$$\left(\frac{S}{N}\right)_{\text{pol}}^2 = \sum_l \frac{(2l+1) \hat{C}_l^{T_{\text{isw}}}}{C_l^{T_{\text{prim}}} - (C_l^{T_{\text{prim},E_{\text{cmb}}}})^2 / C_l^{E_{\text{cmb}}}}. \quad (31)$$

As we said before, the signal-to-noise ratio depends on the specific LSS realisation in our Universe via  $\hat{C}_l^{T_{\text{isw}}}$ . We can infer its probability distribution from the distribution of  $T_{\text{isw}}$  by using the central limit theorem for the distribution of  $(S/N)^2$  and deriving the distribution for  $S/N$  from that (see also Frommert et al. 2008)<sup>2</sup>. We then average the signal-to-noise ratio over this probability distribution in order to compare it to the signal-to-noise ratio of the

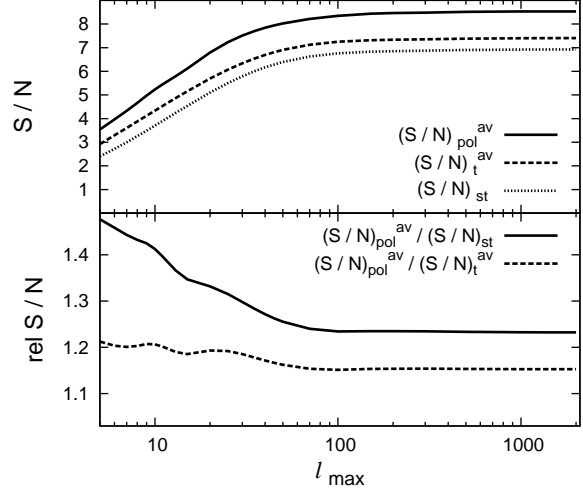


**Figure 4.** Comparison of the cumulative signal-to-noise ratios for  $z_{\text{max}} = 2$ . **Top panel:** Average signal-to-noise ratio of the optimal polarisation method  $(S/N)_{\text{pol}}^{\text{av}}$  (solid), of the optimal temperature-only method  $(S/N)_t^{\text{av}}$  (dashed), and signal-to-noise ratio of the standard method  $(S/N)_{\text{st}}$  (dotted) versus the maximal multipole considered in the analysis. **Bottom panel:** Ratio of the signal-to-noise of the optimal polarisation method with the one of the standard method (solid) and with the one of the optimal temperature-only method (dashed).

standard method and the average signal-to-noise ratio of the optimal temperature-only method, both described in Frommert et al. (2008). Recall that the signal-to-noise ratio one obtains for the standard method is given by

$$\left(\frac{S}{N}\right)_{\text{st}}^2 = \sum_l \frac{(2l+1) C_l^{T_{\text{isw}}}}{C_l^{T_{\text{prim}}} + C_l^{T_{\text{isw}}}}. \quad (32)$$

The cumulative signal-to-noise ratios versus the maximal multipole  $l_{\text{max}}$  used in the analysis are plotted in Fig. 4. Here we have assumed the ideal galaxy survey described above. We see that including the polarisation data in the analysis increases the signal-to-noise ratio by 16 per cent as compared to the optimal temperature-only method, and by 23 per cent as compared to the standard method. Note that we only included the linear ISW effect in Fig. 4. Beyond a multipole of about  $l \approx 100$ , non-linear effects start to play a crucial role (Cooray 2002), which could change the plot for  $l > 100$ . However, we see that for the linear ISW effect, there is hardly any contribution for such high multipoles.

Let us now look at the enhancement of the signal-to-noise ratio for shallower LSS surveys. We use the same approximation as in Frommert et al. (2008), i.e. we introduce a sharp cut-off in redshift and redefine everything beyond that redshift as primordial fluctuations. This introduces a correlation between what we consider the ISW and primordial fluctuations, which we would not have if we had used a proper Wiener filter based template  $T_\tau$  for redefining  $T_{\text{isw}}$ . However, for getting a rough picture of the redshift dependence, this approximation is good enough<sup>3</sup>. We plot the redshift-dependence of the signal-to-noise ratios of the three methods in Fig. 5. We also plot the ratio of the signal-to-noise of the optimal polarisation method with the one of the standard method (solid)

<sup>2</sup> This will provide accurate results for multipoles  $l \gg 1$ , however, is a coarse approximation in the regime  $l \sim 1$ .

<sup>3</sup> The ratio of this neglected coupling to the template strength gets large for small  $z_{\text{max}}$ . Our estimates are therefore less accurate in this regime.

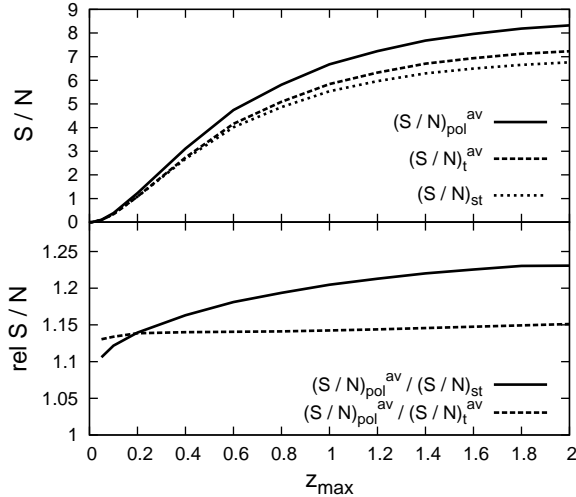


**Figure 5.** Comparison of the signal-to-noise ratios versus the maximal redshift  $z_{\max}$  of the galaxy survey. **Top panel:** Average signal-to-noise ratio of the optimal polarisation method  $(S/N)_{\text{pol}}^{\text{av}}$  (solid), of the optimal temperature-only method  $(S/N)_{\text{t}}^{\text{av}}$  (dashed) and signal-to-noise ratio of the standard method  $(S/N)_{\text{st}}$  (dotted). **Bottom panel:** Ratio of the signal-to-noise of the optimal polarisation method with the one of the standard method (solid) and with the one of the optimal temperature-only method (dashed). We see that with polarisation data included, the signal-to-noise is significantly enhanced even for low redshifts.

and with the one of the optimal temperature-only method (dashed). Note that the enhancement of the signal-to-noise ratio w.r.t. the optimal temperature-only method is almost constant in redshift. This is quite clear from the fact that we have reduced the *primordial* noise with the polarisation data, and neither the primordial noise nor the reduction of the latter depend on redshift. Therefore, the reduction of the noise from including polarisation data is always the same, independent of how deep in redshift our survey goes, and the signal-to-noise ratio is already significantly enhanced for currently available surveys. For example, for a maximal redshift of  $z_{\max} \approx 0.3$ , which is the maximal redshift for the SDSS main galaxy sample, we have a better signal-to-noise by about 16 per cent as compared to the standard method. The additional enhancement for higher redshifts of our signal-to-noise ratio w.r.t. the standard method comes from working conditional on the galaxy data, as we have described in detail in Frommert et al. (2008).

## 5 CONCLUSIONS

The detection of secondary effects on the CMB remains a challenge, because the amplitudes of these effects are much smaller than those of primordial CMB fluctuations. The techniques for detecting such secondary signals are all based on the existing cross-correlation between the LSS and the signal in question. However, in all of these studies, chance correlations of primordial CMB fluctuations with the LSS are the dominant source of noise in the analysis.

We have presented a way of reducing the noise coming from primordial temperature fluctuations by simply subtracting the part of the temperature map which is known from the polarisation data. Effectively, only the unknown part of the temperature fluctuations then contributes to the variance of the signal estimate.

As presented here, our method can be generically applied to

all secondary effects. However, in this work we have used a Gaussian approximation for the uncertainty in the signal template, which may not be optimal for effects on smaller scales, such as the RS effect, the kinetic SZ effect or lensing. We leave the extension of our method to non-Gaussian noise models for future work.

We calculated the achievable reduction in primordial noise for perfect (noiseless) data using the example of the ISW effect, and obtained a signal-to-noise ratio of up to 8.5. This corresponds to an enhancement of the signal-to-noise ratio by 16 per cent as compared to our optimal temperature-only method, independent of the depth of the LSS survey. In comparison to the standard method, the signal-to-noise ratio is enhanced by 23 per cent for a full-sky galaxy survey which goes out to a redshift of at least two. When using the SDSS main galaxy sample, which has a maximal redshift of about  $z_{\max} \approx 0.3$ , our signal-to-noise ratio is still enhanced by about 16 per cent as compared to the standard method.

The variance reduction achieved with this method will significantly improve the detection of all kinds of secondary effects on the CMB, where a spatial template constructed from non-CMB data can be created. This stresses the importance of accurate measurements of primordial polarisation fluctuations even for non-primordial signal detection and analysis. The upcoming Planck Surveyor Mission, as well as more future experiments like PolarBear<sup>4</sup> or CMBPol<sup>5</sup> will allow us to benefit from polarisation for the detection of secondary CMB signals in the way presented in this work.

## ACKNOWLEDGMENTS

The authors would like to thank Martin Reinecke and André Waelkens for their extensive help with HEALPix. We would also like to thank Simon D. M. White, Cheng Li and Thomas Riller for useful discussions and comments. We acknowledge the use of the HEALPix package and CMBEASY.

## REFERENCES

- Afshordi N., 2004, *Phys. Rev. D*, 70, 083536
- Baumann D., Cooray A., Dodelson S., Dunkley J., Fraisse A. A., Jackson M. G., Kogut A., Krauss L. M., Smith K. M., Zaldarriaga M., 2008, ArXiv e-prints
- Boughn S., Crittenden R., 2004, *Nature*, 427, 45
- Boughn S. P., Crittenden R. G., Turok N. G., 1998, *New Astronomy*, 3, 275
- Cooray A., 2002, *Phys. Rev. D*, 65, 083518
- Cooray A., Melchiorri A., 2006, *Journal of Cosmology and Astro-Particle Physics*, 1, 18
- Crittenden R., 2006, <http://www-astro-theory.fnal.gov/Conferences/ECcmbC/PresentationFiles/RobertCrittenden.ppt>, <http://www-astro-theory.fnal.gov/Conferences/ECcmbC/ECcmbCagenda.html>
- Doran M., 2005, *Journal of Cosmology and Astro-Particle Physics*, 10, 11
- Enßlin T. A., Frommert M., Kitaura F. S., 2008, submitted to *Phys. Rev. D*, astro-ph/0806.3474
- Frommert M., Enßlin T. A., Kitaura F. S., 2008, *MNRAS* in press

<sup>4</sup> <http://bolo.berkeley.edu/polarbear/index.html>

<sup>5</sup> Baumann et al. (2008), <http://cmbpol.uchicago.edu>

- Giannantonio T., Scranton R., Crittenden R. G., Nichol R. C., Boughn S. P., Myers A. D., Richards G. T., 2008, *Phys. Rev. D*, 77, 123520
- Górski K. M., Hivon E., Banday A. J., Wandelt B. D., Hansen F. K., Reinecke M., Bartelmann M., 2005, *ApJ*, 622, 759
- Granett B. R., Neyrinck M. C., Szapudi I., 2008, *astro-ph/0805.2974*
- Haehnelt M. G., Tegmark M., 1996, *MNRAS*, 279, 545
- Hernández-Monteagudo C., 2008, *A&A*, 490, 15
- Ho S., Hirata C., Padmanabhan N., Seljak U., Bahcall N., 2008, *Phys. Rev. D*, 78, 043519
- Jaffe A. H., 2003, *New Astronomy Review*, 47, 1001
- Komatsu E., et al., 2008, *astro-ph/0803.0547*
- Lewis A., Challinor A., 2006, *Phys. Rep.*, 429, 1
- Maturi M., Dolag K., Waelkens A., Springel V., Enßlin T., 2007a, *A&A*, 476, 83
- Maturi M., Enßlin T., Hernández-Monteagudo C., Rubiño-Martín J. A., 2007b, *A&A*, 467, 411
- Rassat A., Land K., Lahav O., Abdalla F. B., 2006, *astro-ph/0610911*
- Rees M. J., Sciama D. W., 1968, *Nature*, 217, 511
- Sachs R. K., Wolfe A. M., 1967, *ApJ*, 147, 73
- Schäfer B. M., Pfrommer C., Hell R. M., Bartelmann M., 2006, *MNRAS*, 370, 1713
- Sunyaev R. A., Zeldovich Y. B., 1972, *Comments on Astrophysics and Space Physics*, 4, 173
- Sunyaev R. A., Zeldovich Y. B., 1980, *ARA&A*, 18, 537
- Tauber J. A., 2000, *Astrophysical Letters Communications*, 37, 145
- Waelkens A., Maturi M., Enßlin T., 2008, *MNRAS*, 383, 1425
- Zaldarriaga M., 1997, *Phys. Rev. D*, 55, 1822
- Zhang P., 2006, *ApJ*, 647, 55

## APPENDIX A: PROOF OF THE FACTORIZATION OF THE LIKELIHOOD

We now explicitly prove the factorization of the likelihood in eq. (21) into a reduced temperature part and a polarisation part, as given in eq. (23). We will do this for the more general case that we not only have a signal template  $T_\tau$  for the temperature part, but also a non-zero template  $E_\tau$  for the polarisation part. In this case, the covariance matrix is

$$\tilde{C}(l) = \begin{pmatrix} C_l^{\Delta T_{\text{obs}}} & C_l^{\Delta T_{\text{obs}}, \Delta E_{\text{obs}}} \\ C_l^{\Delta T_{\text{obs}}, \Delta E_{\text{obs}}} & C_l^{\Delta E_{\text{obs}}} \end{pmatrix}, \quad (\text{A1})$$

instead of the simplified one given in eq. (20). Here,  $\Delta E_{\text{obs}}$  is defined as  $\Delta E_{\text{obs}} \equiv E_{\text{obs}} - E_\tau$ . The inverse of the covariance matrix is given by

$$\tilde{C}(l)^{-1} = \frac{1}{C_l^{\Delta T_{\text{obs}}} C_l^{\Delta E_{\text{obs}}} - \left(C_l^{\Delta T_{\text{obs}}, \Delta E_{\text{obs}}}\right)^2} \times \begin{pmatrix} C_l^{\Delta E_{\text{obs}}} & -C_l^{\Delta T_{\text{obs}}, \Delta E_{\text{obs}}} \\ -C_l^{\Delta T_{\text{obs}}, \Delta E_{\text{obs}}} & C_l^{\Delta T_{\text{obs}}} \end{pmatrix}. \quad (\text{A2})$$

We first rewrite the exponent of  $\mathcal{G}(a_{lm}^d - a_{lm}^\tau, \tilde{C}(l))$  in eq. (21) by inserting the inverse of  $\tilde{C}(l)$ :

$$\begin{aligned} & \left(a_{lm}^{T_{\text{obs}}} - a_{lm}^{T_\tau}, a_{lm}^{E_{\text{obs}}} - a_{lm}^{E_\tau}\right) \tilde{C}(l)^{-1} \left(a_{lm}^{T_{\text{obs}}} - a_{lm}^{T_\tau}, a_{lm}^{E_{\text{obs}}} - a_{lm}^{E_\tau}\right)^\dagger \\ &= \left[ \left| a_{lm}^{\Delta T_{\text{obs}}} \right|^2 - 2 \left( C_l^{\Delta T_{\text{obs}}, \Delta E_{\text{obs}}} / C_l^{\Delta E_{\text{obs}}} \right) \text{Re} \left( a_{lm}^{\Delta E_{\text{obs}}} a_{lm}^{\Delta T_{\text{obs}}} \right) \right. \end{aligned}$$

$$\begin{aligned} & \left. + \left( C_l^{\Delta T_{\text{obs}}} / C_l^{\Delta E_{\text{obs}}} \right) \left| a_{lm}^{\Delta E_{\text{obs}}} \right|^2 \right] \\ & / \left[ C_l^{\Delta T_{\text{obs}}} - \left( C_l^{\Delta T_{\text{obs}}, \Delta E_{\text{obs}}} \right)^2 / C_l^{\Delta E_{\text{obs}}} \right] \\ &= \frac{\left| a_{lm}^{\Delta T_{\text{obs}}} - \left( C_l^{\Delta T_{\text{obs}}, \Delta E_{\text{obs}}} / C_l^{\Delta E_{\text{obs}}} \right) a_{lm}^{\Delta E_{\text{obs}}} \right|^2}{C_l^{\Delta T_{\text{obs}}} - \left( C_l^{\Delta T_{\text{obs}}, \Delta E_{\text{obs}}} \right)^2 / C_l^{\Delta E_{\text{obs}}}} \\ & + \frac{\left| a_{lm}^{\Delta E_{\text{obs}}} \right|^2}{C_l^{\Delta E_{\text{obs}}}} \\ & \equiv \frac{\left| a_{lm}^{T_{\text{red}}} - a_{lm}^{T_\tau} \right|^2}{C_l^{\text{red}}} + \frac{\left| a_{lm}^{E_{\text{obs}}} - a_{lm}^{E_\tau} \right|^2}{C_l^{\Delta E_{\text{obs}}}} \end{aligned} \quad (\text{A3})$$

where we have completed the square in the second last step and used a generalised definition of the reduced temperature map and power spectrum, which we had introduced in eq. (22), in the last step. Similarly, we can decompose the determinant of  $\tilde{C}(l)$ :

$$\begin{aligned} \left| \tilde{C}(l) \right| &= C_l^{\Delta T_{\text{obs}}} C_l^{\Delta E_{\text{obs}}} - \left( C_l^{\Delta T_{\text{obs}}, \Delta E_{\text{obs}}} \right)^2 \\ &\equiv C_l^{\text{red}} C_l^{\Delta E_{\text{obs}}}. \end{aligned}$$

Inserting eqs (A3) and (A4) into  $\mathcal{G}(a_{lm}^d - a_{lm}^\tau, \tilde{C}(l))$  allows us to write

$$\begin{aligned} \mathcal{G}(a_{lm}^d - a_{lm}^\tau, \tilde{C}(l)) &= \mathcal{G}(a_{lm}^{T_{\text{red}}} - a_{lm}^{T_\tau}, C_l^{\text{red}}) \\ &\quad \times \mathcal{G}(a_{lm}^{E_{\text{obs}}} - a_{lm}^{E_\tau}, C_l^{\Delta E_{\text{obs}}}). \end{aligned} \quad (\text{A4})$$

In the case of the polarisation template  $E_\tau$  being zero, this expression reduces to the one in eq. (23).